Polydisperse Mixture Adsorption Kinetics

Ramachandran Muralidhar and Julian Talbot
School of Chemical Engineering, Purdue University, West Lafayette, IN 47907

We present a theoretical study of the adsorption kinetics of particles with a continuous distribution of sizes. If the particles interact with short-ranged forces, the diminishing rate of adsorption with increasing surface coverage can be attributed to a geometrical blocking effect of the preadsorbed particles. We exploit the fact that at low coverages the blocking effects result from isolated adsorbed particles to develop an analytic description of the adsorption kinetics using a moment expansion approach. We evaluate the time-dependent surface coverage, density and the average size of the adsorbed particles and compare these quantities with those of the bulk phase. The effect of desorption is studied by introducing a size-independent desorption constant, and the corresponding adsorption equilibria properties, which are valid at low coverages, are derived. Simulation results for irreversible adsorption are obtained and compared with the theoretical predictions.

Introduction

Adsorption processes are of fundamental importance in a wide range of applications including filtration, water cleansing, and chromatography. For references and a review of some theoretical approaches to the adsorption of colloidal particles, the reader is referred to Hirtzel and Rajagopalan (1985) and Van den Ven (1989). Although there have been numerous theoretical studies of the initial adsorption rate on clean surfaces, much work is still required to develop quantitative descriptions at finite surface coverages. The Langmuir equation and its modifications are firmly entrenched as the model for adsorption kinetics. These models, however, may not be applicable to systems where the adsorption is not localized on distinct sites.

The diminishing rate of adsorption with increasing surface coverage may be explained by the blocking effect of the adsorbed molecules. For a monodisperse adsorbent, one may write a general kinetic equation in the form:

$$\frac{d\theta}{dt} = k_a c_0 \phi(\theta) - k_d \theta \tag{1}$$

where k_a and k_d are the adsorption and desorption constants, respectively, c_0 is the bulk concentration, and θ is the surface coverage. The exclusion effects are represented by the *available surface function* $\phi(\theta)$. Clearly, $\phi(0) = 1$ and ϕ decreases monotonically with increasing coverage. A useful first approximation is to regard the blocking effect as being purely geometrical in nature. That is, for a given configuration of adsorbed molecules, a certain fraction of the surface is inaccessible to the center of a new molecule: if this molecule were to land in the inaccessible area, an overlap would result with at least one of the previously adsorbed molecules. Such an event is highly energetically unfavorable and assumed not to occur (in this work we do not consider the possibility of multilayer formation). The simplest reasonable form for the available surface function is $\phi(\theta) = 1 - \theta$, that is, the Langmuir model. This equation can easily be derived by assuming that each adsorbing molecule occupies one adsorption site, and the sites are independent. The available surface is then just the fraction of unoccupied sites. For large molecules, however, proteins or latex spheres, for example, this picture is no longer valid (Schaaf and Talbot, 1989). To illustrate this point, consider the adsorption of spheres of diameter σ onto a planar surface. Associated with each adsorbed sphere is an exclusion circle of radius σ which cannot be occupied by the center of a new sphere. On a nearly empty surface, the exclusion circles are mostly isolated and the available surface at density ρ is $1 - \pi\sigma^2\rho$, or in terms of the coverage, $\theta = \pi\sigma^2\rho/4$, this is $1 - 4\theta$. With increasing coverage, overlap between two or more exclusion circles becomes more likely. To incorporate these effects it is useful to write ϕ as a power series:

$$\phi = 1 + a_1\theta + a_2\theta^2 + a_3\theta^3 + \ldots \tag{2}$$

Current address of R. Muralidhar: Mobil Research and Development Corporation, Paulsboro, NJ 08066.

To proceed, one must know something about the nature of the adsorption process. At one extreme is the random sequential adsorption (RSA) process where no relaxation of the surface configuration is possible: that is, the adsorbed molecules remain permanently fixed in place with no surface diffusion or desorption ($k_d=0$). It has been proposed that the RSA model may describe the irreversible adsorption of certain proteins (Feder, 1980). On the other hand, if the adsorbed molecules are sufficiently mobile, the surface configuration will relax to equilibrium between each successive addition of a new particle. All real adsorption processes lie between these two extremes. An interesting and important observation due to Widom (1966) is that the coefficients a_1 and a_2 in the above expansion are the same for equilibrium and RSA configurations in the absence of external fields. That is, at sufficiently low coverages, it is impossible to distinguish configurations generated by a purely irreversible adsorption from those generated by an equilibrium process. At higher coverages, however, the differences are significant. For the adsorption of hard spheres we have already demonstrated that $a_1=-4$. It can be shown that either directly or by relating ϕ to virial expansion of the hard disk fluid, $a_2=6\sqrt{3}/\pi$. Higher terms must be computed for the specific process. For example, $a_3^{rsa}=1.4069$ and $a_3^{eq}=2.4041$ (Schaaf and Talbot, 1989).

The purpose of this article is to extend some of the above ideas to systems in which there is a continuous distribution of adsorbent diameters, as might be found, for example, in a polydisperse latex solution or filtration processes. It is possible to write down a formal expression for ϕ in terms of the n-particle distribution functions for the adsorbed molecules (Tarjus et al., 1991). However, here we shall concern ourselves solely with the coefficient a_1. By neglecting higher-order terms in Eq. 2, one may obtain analytic or semianalytic solutions for the adsorption kinetics or adsorption isotherm. Although the range of validity of the solutions is expected to be limited, they do describe both reversible and irreversible adsorption processes. As will be shown, the equations that we develop accurately describe the *initial* adsorption kinetics or the equilibrium isotherm, when the surface coverage is small. In the monodisperse system, it is of no consequence whether we regard the adsorbent molecules as disks or spheres. This distinction, however, is important when different sized particles are present (Talbot and Schaaf, 1989).

In this article, we derive the analog of Eq. 1 for a continuous distribution of particle diameters and discuss the *moment method* for obtaining solutions for transient and equilibrium situations. Both size-independent and size-dependent adsorption rate coefficients are considered. And then, the specific cases of sphere and disk geometries are analyzed. Subsequently, the results of a numerical simulation of the adsorption of a polydisperse mixture are compared with the predictions.

Theory

The equivalent of Eq. 1 in the polydisperse case is:

$$\frac{\partial\rho(r;t)}{\partial t}=k_a(r)c_0(r)\phi(r;t)-k_d(r)\rho(r;t) \tag{3}$$

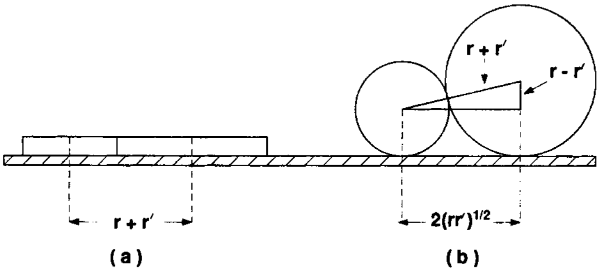

Figure 1. Exclusion effects for (a) hard disks and (b) hard spheres.

where $\rho(r;t)dr$ is the surface density of adsorbed molecules of radius between r and $r+dr$, $c_0(r)dr$ is the corresponding bulk concentration, $k_a(r)$ and $k_d(r)$ are the adsorption and desorption rates for particles of radius r, respectively, and $\phi(r;t)$ is the available surface function for an incoming molecule of radius r. A convenient dimensionless form of Eq. 2 is presented in the Appendix. The fractional available area accessible to an incoming particle of radius r is to first order in density:

$$\phi(r;t)=1-\int_0^\infty a(r,r')\rho(r';t)dr' \tag{4}$$

where $a(r,r')$ is the area excluded by an adsorbed particle of radius r' to the incoming particle of radius r. We emphasize that Eq. 2 assumes additivity of excluded areas, which is strictly valid *only* at small coverages. The exact nature of even the pair exclusion area is not known. For particles interacting with hard-core excluded volume interactions, it depends on the geometry of the adsorbed species. For simple two-dimensional disks, one may write (Figure 1a):

$$a^{(2D)}(r,r')=\pi(r+r')^2 \tag{5}$$

while for three-dimensional rigid spheres (Figure 1b):

$$a^{(3D)}(r,r')=4\pi rr' \tag{6}$$

Note that both the above expressions are symmetric in r and r'. However, the above symmetry condition is not valid in general. When we consider particles interacting with a short-range potential, it is more appropriate for short times that $a(r,r')$ be given by Eq. 5 for $r>r'$ and by Eq. 6 for $r<r'$. This is because a smaller particle of radius r would have to execute a complex rolling motion on the surface of the larger particle of radius r' to achieve the configuration shown in Figure 1b. However, for large times or under conditions close to equilibrium, such a configuration is possible as a result of thermal motion: $a(r,r')$ is then given by Eq. 6.

We note at this point that the Langmuir equation may be obtained by setting $a(r,r')=\pi r'^2$ to yield:

$$\phi(r,t)=1-\theta(t) \tag{7}$$

where

$$\theta(t)=\int_0^\infty \pi r'^2\rho(r',t)dr' \tag{8}$$

Thus, in the Langmuir approximation, the adsorption rate of a particle is independent of its size—clearly a crude approximation.

In general, the adsorption and desorption rate coefficients depend on the radius of the particle and the absolute temperature T. The adsorption kinetics are determined by the detailed nature of the adsorbing particle's thermal motion in the bulk and the particle-surface interactions contained in ϕ. For diffusion-limited adsorption, k_a is proportional to the diffusivity of the particle, which is in turn proportional to the absolute temperature T and the inverse of the hydrodynamic radius. If the trajectories of the adsorbing particles are ballistic, then k_a is proportional to the mean thermal speed and hence scales as $\sqrt{T/m}$. In general, we assume:

$$k_a(r)=\chi_a(T)r^{\mu} \tag{9}$$

where the power-law exponent, μ, is generally less than or equal to zero. Similarly, for the desorption constant we assume:

$$k_d(r)=\chi_d(T)r^{\nu} \tag{10}$$

where $\nu\leq 0$.

On substituting Eqs. 4, 9 and 10 in Eq. 3, one obtains:

$$\frac{\partial\rho(r;s)}{\partial s}=r^{\mu}c_0(r)\left[1-\int_0^{\infty}a(r,r')\rho(r',s)dr'\right]-kr^{\nu}\rho(r,s) \tag{11}$$

where $k(T)=\chi_d/\chi_a$ and $s=\chi_a(T)t$ is a rescaled time. In the cases where $\mu=\nu$, the parameter $1/k$ corresponds to the Henry's law constant. A complete solution of the above integrodifferential equation is difficult to obtain. A convenient method that exploits the polynomial nature of the available surface function to first order in density is that of moments, in which one seeks not the complete surface distribution function, but only its moments. The pth surface moment is defined by:

$$m_p(s)=\int_0^{\infty}r^p\rho(r,s)dr,\ p=0,1,2\ldots \tag{12}$$

Several quantities of experimental interest are readily obtained from these moments. Thus, the zeroth moment corresponds to the total number density of adsorbed particles, while the coverage θ is given by:

$$\theta=\pi m_2 \tag{13}$$

The average size of the adsorbed particles is given by the normalized first moment:

$$\langle r\rangle=\frac{m_1}{m_0} \tag{14}$$

and the mean squared fluctuation is given by:

$$\delta^2=\frac{m_2}{m_0}-\left(\frac{m_1}{m_0}\right)^2 \tag{15}$$

The moments of the bulk-phase concentration are similarly defined by:

$$n_p=\int_0^{\infty}r^pc_0(r)dr,\quad p=0,1,2\ldots \tag{16}$$

We now apply the method of moments to the 2D (disks) situation. Substituting Eq. 5 in Eq. 11, multiplying by r^p and integrating over r we obtain:

$$\frac{dm_p(s)}{ds}=n_{p+\mu}-\pi[n_{p+2+\mu}m_0(s)+n_{p+\mu}m_2(s)+2n_{p+1+\mu}m_1(s)]-km_{p+\nu}(s) \tag{17}$$

Similarly for the 3D (sphere) case with $a(r,r')$ given by Eq. 6, one finds:

$$\frac{dm_p(s)}{ds}=n_{p+\mu}-4\pi n_{p+\mu+1}m_1-km_{p+\nu} \tag{18}$$

In both cases, the original integrodifferential equation is replaced by an infinite set of first-order differential equations. As we have already remarked, however, the interesting experimental quantities are simply related to the low-order moments.

Two slightly different approaches are required to solve Eqs. 17 and 18. The latter is somewhat simpler, and we will develop a number of analytic solutions and consider the more involved two-dimensional case in the following sections. As an illustration of the method, we apply our solutions to a bulk-phase distribution given by:

$$c_0(r)=re^{-r} \tag{19}$$

for which $n_0=1$, $n_1=2$, $n_2=6$.

Solutions for Spherical Geometry

Adsorption kinetics with k = C

For simplicity, we consider the case where the exclusion area is given by Eq. 6. The mixed case, Eqs. 5 and 6, is expected to be qualitatively similar. It is evident that all the moments are completely determined in terms of the first moment which satisfies the equation:

$$\frac{dm_1(s)}{ds}=n_{1+\mu}-4\pi n_{2+\mu}m_1(s) \tag{20}$$

For a vanishing initial condition (empty surface at $s=0$), the above yields:

$$m_1(s)=\frac{n_{1+\mu}}{4\pi n_{2+\mu}}[1-\exp(-4\pi n_{2+\mu}s)] \tag{21}$$

Incorporating the above in Eq. 20 and solving for the other moments, we obtain:

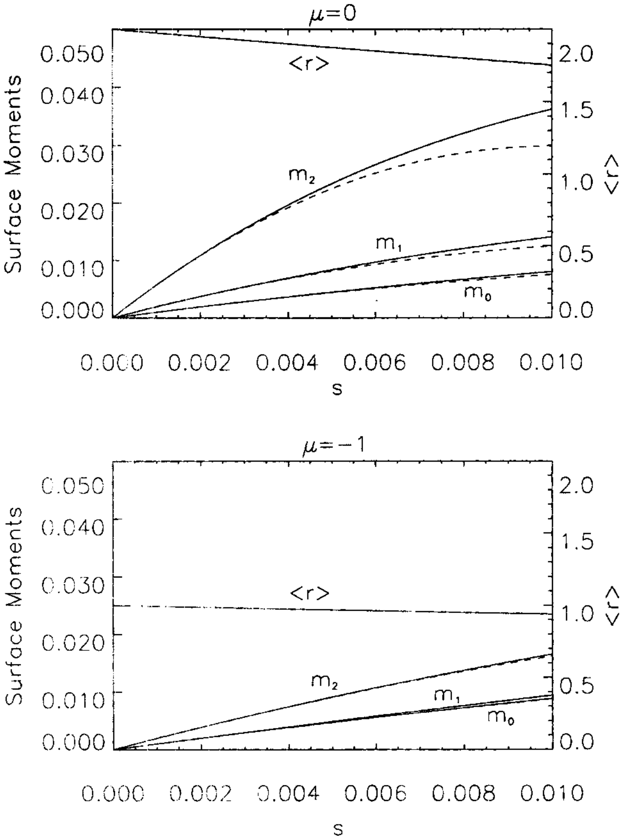

Figure 2. RSA kinetics for rolling hard spheres as a function of the rescaled time s with: (a) size-independent adsorption kinetics coefficients ($\mu=0$); (b) adsorption kinetics proportional to the inverse particulate radii.

The average radius of the adsorbed spheres is computed from $\langle r\rangle = m_1/m_0$. The solid line shows values computed from the analytic solutions (Eq. 22), while the dashed lines show the short time expansions of these solutions (Eqs. 23 and 24). The bulk distribution of particle sizes is given by Eq. 19.

$$m_p(s) = \left[n_{p+\mu} - \frac{n_{p+1+\mu} n_{1+\mu}}{n_{2+\mu}} \right] s + \frac{n_{p+1+\mu} n_{1+\mu}}{4\pi n_{2+\mu}^2} [1 - \exp(-4\pi n_{2+\mu} s)], \quad p = 0,1,2,\ldots \tag{22}$$

It is interesting to examine the short time behavior of this solution. Expanding the exponential to second order in s, one has:

$$m_p(s) = n_{p+\mu} s - 2\pi n_{p+1+\mu} n_{1+\mu} s^2 + O(s^3) \tag{23}$$

and

$$\frac{m_p(s)}{m_0(s)} = \frac{n_{p+\mu}}{n_\mu} + \frac{2\pi n_{\mu+1}}{n_\mu^2} (n_{\mu+1} n_{p+\mu} - n_\mu n_{\mu+1+p}) s + O(s^2) \tag{24}$$

Thus, at the onset of the adsorption process, the normalized surface moments are very simply related to normalized moments of the bulk phase. In the case of size-independent adsorption coefficient ($\mu=0$), these two quantities are equal, while for preferential adsorption due to size-specific kinetics ($\mu \neq 0$), the normalized moments of the two phases are unequal. From Eq. 24, it is clear that the properties of the surface size distribution such as the average size are identical to the $s=0$ limit for small s [more specifically to $O(s)$]. This is because the surface is practically empty and the blocking effects are negligible. With increasing time, however, the $O(s^2)$ terms become important, and the properties of the normalized moments of the surface deviate from their initial values.

Figure 2 depicts the various moments for the adsorbed phase for a mass-independent adsorption coefficient ($\mu=0$) and a bulk distribution given by Eq. 19. The zeroth moment represents the total number of adsorbed particles and the coverage increase with time. At time $s=0^+$, the adsorbent surface is empty and there are no blocking effects. The first and second normalized moments of the adsorbed phase are then equal to the bulk values. With increasing time, the surface coverage and hence the blocking effects increase. Because this shielding effect is smaller for smaller particles, they are adsorbed with greater facility compared with larger ones. Figure 2 also shows the temporal evolution of the moments for the case of adsorption coefficients determined by Stokes-Einstein diffusion ($\mu = -1.0$) and the same distribution in the bulk phase. In this case, even at $s=0^+$, the greater mobility of the smaller particles causes the surface moments to deviate considerably from the bulk values. The exclusion effects are smaller because the surface population is rich in the smallest particles. This, along with the rapid movement of small particles toward the surface, causes the moments to decay more slowly than before.

Equilibrium

At equilibrium, the isotherm is obtained by setting the left-hand side of Eq. 18 equal to zero to obtain:

$$n_{p+\nu} = 4\pi n_{p+\mu+1} m_1 + k m_{p+\nu} \tag{25}$$

Setting $p = 1-\nu$, solving for the first moment m_1 and then for arbitrary moments, one finds:

$$k m_p = n_{\mu-\nu+p} - \frac{4\pi n_{\mu-\nu+1+p} n_{\mu-\nu+1}}{k + 4\pi n_{\mu-\nu+2}} \tag{26}$$

Figure 3 depicts the equilibrium moments for different values of the parameter k for the case $\mu=\nu$. The values of k were chosen to yield small surface coverages. As k decreases, the relative rate of adsorption over desorption increases resulting in an increase of both the surface density and surface coverage. The blocking effects become increasingly important, and the surface moments decrease from their bulk values. Unlike in the dynamic situation considered in the previous section, the case of mass-dependent and mass-independent kinetics yield identical results when $\mu=\nu$.

Solutions for Disk Geometry

The extra complexity arises here because of the couping of the moments in Eq. 17. For irreversible adsorption, $k=0$, it is evident from Eq. 17 that all the moments greater than two are completely determined once the lower moments are known.

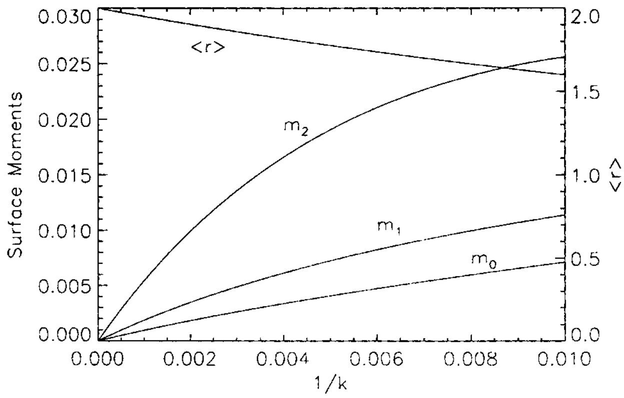

Figure 3. Equilibrium surface moments for rolling hard spheres as a function of the equilibrium constant, *k*.

The values are computed from Eq. 26 assuming a bulk distribution given by Eq. 19 and $\mu=\nu$. The results are only expected to be reliable for very small k.

Thus, it is only necessary to solve explicitly for moments lower than three. The problem may be written in matrix notation as:

$$\frac{dm}{ds}=n-\pi N\cdot m \tag{27}$$

where

$$m=[m_0,\ m_1,\ m_2],\quad n=[n_\mu,\ n_{1+\mu},\ n_{2+\mu}] \tag{28}$$

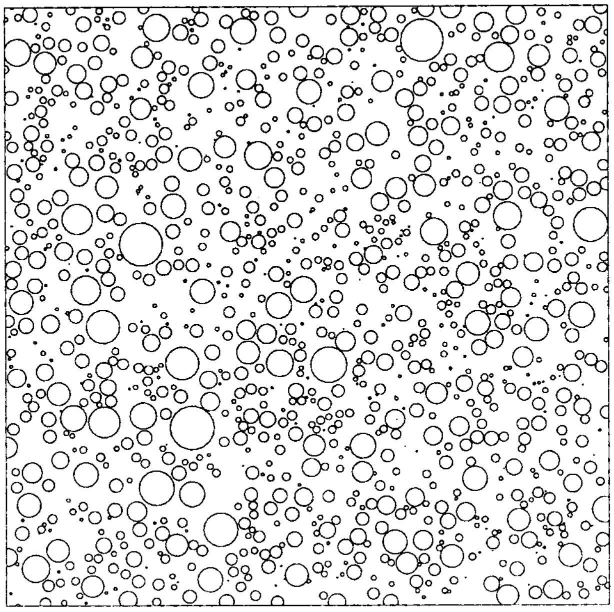

Figure 4. Configuration produced by the irreversible adsorption of polydisperse disks with a bulk distribution given by Eq. 19.

The rescaled time is $s = 0.096$, corresponding to 3,000 placement attempts in the cell of side $L = 176.4$.

and

$$N=\begin{pmatrix} n_{2+\mu} & 2n_{1+\mu} & n_\mu \\ n_{3+\mu} & 2n_{2+\mu} & n_{1+\mu} \\ n_{4+\mu} & 2n_{3+\mu} & n_{2+\mu} \end{pmatrix} \tag{29}$$

The above may be readily integrated numerically using a library routine. In addition, we find the following (exact) short-time behavior for the moments (with $\mu=0$):

$$m_p(s)=n_p s-\frac{\pi}{2}\,(n_{p+2}n_0+n_p n_2+2n_{p+1}n_1)s^2+O(s^3) \tag{30}$$

and

$$\frac{m_p(s)}{m_0(s)}=\frac{n_p}{n_0}+\frac{\pi}{2n_0^2}\,(n_p n_2 n_0+2n_p n_1^2-n_0^2 n_{p+2}-2n_{p+1}n_1 n_0)s+O(s^2) \tag{31}$$

Comparison of the above with Eq. 24 indicates clearly that the solutions are qualitatively similar for short times.

The solution procedure for the equilibrium surface moments is similar to that for the kinetics, except that one now solves three linear simultaneous equations for m_0, m_1 and m_2, from which all other moments may be computed. Again, we have found that the solutions are qualitatively similar to the case of spheres considered in the previous section.

Computer Simulation of Adsorption

To establish the range of validity of the expressions developed in the previous sections, we have simulated the irreversible adsorption of a polydisperse mixture of disks on a planar surface. The simulation algorithm is similar to those used in earlier investigations of the RSA process (Hinrichsen et al., 1986; Schaaf and Talbot, 1989).

The simulations are performed in a square cell of side L with periodic boundary conditions. We specify the system size by fixing the ratio of the average disk area to the system area: $\pi\langle r^2\rangle/L^2$. For the results reported here, we used a value of 0.006 for this parameter which corresponds to a box side of $L=176.4$ (arbitrary units). The simulation consists of a number of attempts to introduce new disks onto the surface. At each step, a trial position for a new disk is selected from a uniform, random distribution using a linear congruential generator. The disk radius is sampled from Eq. 19 using an algorithm originally proposed by Von Neumann (for example, Allen and Tildesley, 1987). The trial disk is accepted only if it does not overlap with any previously adsorbed disk. The simulation time corresponding to the rescaled time s of the theoretical expressions is N_A/L^2, where N_A is the number of attempts that have been made to add disks.

Figure 4 shows a typical configuration after 3,000 placement attempts (or a reduced time of 0.096). Of these, 1,145 were successful, and the resulting configuration has a coverage of 31.1 %. The distribution of diameters of the adsorbed particles at two different times is shown in Figure 5. As expected, the surface becomes progressively richer in smaller particles as the total surface coverage increases.

In Figure 6 we compare the moments as computed in the simulation with those computed from a numerical solution of

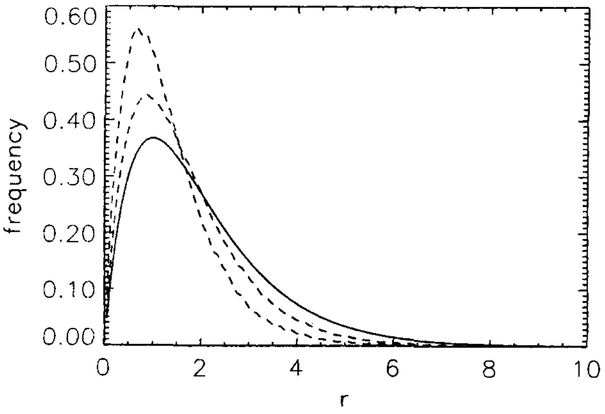

Figure 5. Distribution of adsorbed disk radii (dashed lines) after elapsed rescaled times of $s = 0.043$ and $s = 0.096$.

The latter distribution is the more sharply peaked curve and the solid line is the bulk distribution Eq. 19.

Eq. 27. Note the substantial error in the simulation curves at short times which results from the small number of adsorbed disks and hence poor statistics. Nevertheless, since we know that the surface moments must equal the corresponding bulk moments initially (for size-independent adsorption coefficients), we can see that the theoretical expressions accurately describe the initial slope of the curves. At longer times, however, the differences become significant. In Figure 7 we show the zeroth moments from simulation, from a numerical solution of Eq. 27 and the expansion (Eq. 30). In this case, the solution of Eq. 27 is more accurate.

Finally, Figure 8 shows the total rate of adsorption as a function of time. The simulation result was obtained by numerically differentiating the coverage and hence is somewhat noisy. Both theoretical expressions correctly predict the initial slope. However, since the theory represents the blocking effects only to first order in coverage, differences between the theory and simulation soon appear.

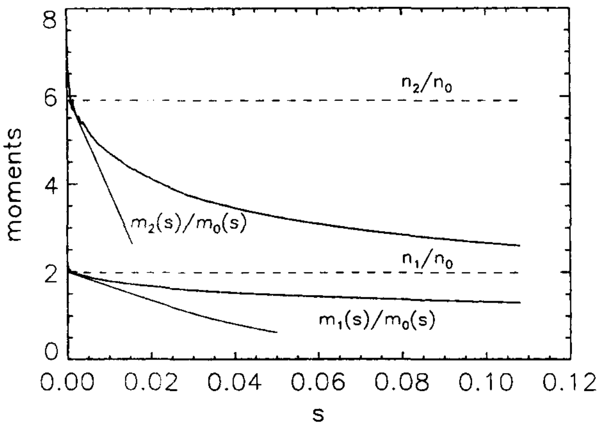

Figure 6. Comparison of the surface moments of adsorbed disks.

They are computed from the simulation (thick lines) and from a numerical solution of Eq. 27 as a function of rescaled time, s. Also shown are the bulk moments, n_p.

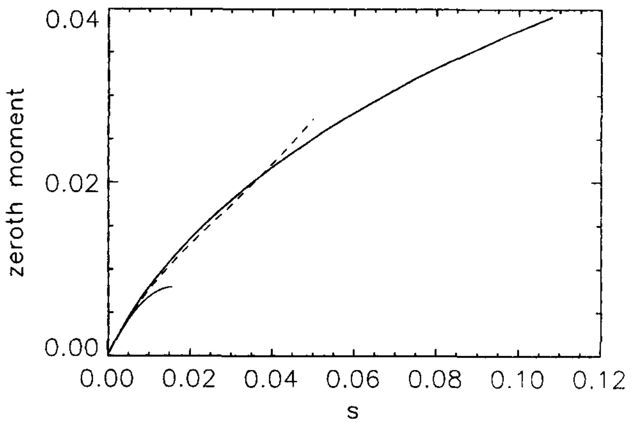

Figure 7. Comparison of the zeroth moment of adsorbed disks.

They are computed from the simulation (thick line) and the theoretical expressions. The dashed line is a numerical solution to Eq. 27, while the thin solid line is computed from Eq. 30.

Discussion

The adsorption of polydisperse mixtures is a phenomenon underlying many natural and industrial processes. However, as this article hopefully illustrates, the development of theories is a complicated task. The present analysis is limited in a number of ways: the particles are assumed to interact via short-ranged hard-core potentials, and only monolayer adsorption at low surface coverages are within the domain of the expansions presented here. At this level of description, however, the equations apply to both reversible and irreversible adsorption.

A comparison with the results of a computer simulation of the RSA of polydisperse hard disks shows that the theory accurately describes the initial rate of adsorption. Indeed, within the framework of the model, the equations are exact in this limit. With increasing coverage, however, the agreement between theory and simulation deteriorates rapidly. Judging

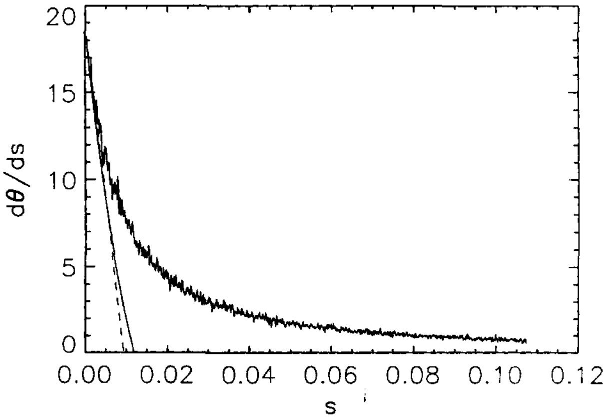

Figure 8. Overall rate of adsorption, $d\theta/ds$, as a function of the rescaled time, s for a mixture of polydisperse disks with a bulk distribution given by Eq. 19.

Jagged line, computer simulation results; smooth solid line, numerical solution of Eq. 27; and dashed line, derivative of Eq. 30.

from the results for the RSA of monodisperse hard spheres (Schaaf and Talbot, 1989), accounting for the exclusion effects to second order in surface density would significantly extend the useful range of the theory without reducing the versatility of the equations: that is, they would still describe both reversible and irreversible adsorption. Such a development is certainly possible, although the resulting expressions will be considerably more complex than those presented here.

We should stress that although the expansions are limited to a description of the initial rate of adsorption, they have a firm theoretical foundation and, as a consequence, are considerably more accurate in describing the initial rate of adsorption than the multicomponent Langmuir equation which sets $\phi_i = 1 - \Sigma\theta_j$. If one can measure the initial rate of adsorption and the moments of the bulk concentration, then one may compute a physically significant adsorption rate constant, $\chi_a(T)$. Although the Langmuir equations may provide a reasonable fit to experimental data, the physical significance of the constants is less clear.

The moment analysis of the adsorption equation reveals that for size-independent kinetic coefficients, the moments of the surface population initially start out at their bulk values, but show deviations as the surface coverage increases. More specifically, the average size of the adsorbed particles is smaller than that of those in the bulk. This is because the blocking effect is less severe for smaller rather than larger particles. In situations where the kinetic coefficients decrease with increasing size, the preferential adsorption of smaller particles is enhanced. Under these conditions, even at very small times, the surface moments are much smaller than the bulk values.

There are a number of interesting questions that are not addressed in this work. In particular, for irreversible adsorption, one would like to understand how the coverage and particle size distribution in the jammed state depend on the bulk concentration and adsorption rates. Meakin and Jullien (1992) have made some progress in this direction. Although the computer simulation is very slow near saturation, it is possible to extrapolate the results to infinite time using exact expressions for the asymptotic kinetics (Tarjus and Talbot, 1991). Development of purely theoretical expressions for the saturation coverage is beyond current capabilities, except in the case of one-dimensional models, that is, the adsorption of polydisperse rods on a line.

A quantitative description of the kinetics of the approach to equilibrium in reversible adsorption would be of great benefit in chromatography. Although one can examine the transient kinetics with the equations presented here, the results would be valid only for very small coverages. We are currently examining reversible adsorption processes at finite coverages with computer simulation.

One effect which is not considered in any of the above and which may be important is the possibility of a change of size or conformation on adsorption. The radius of a flexible molecule on the surface is in general different from that in the bulk. For example, protein folding on surfaces changes their conformation.

Acknowledgment

R. Muralidhar acknowledges the Department of Chemical Engineering at Purdue University for a post doctoral fellowship. J. Talbot acknowledges support from NSF under Grant No. CTS-9011240.

Notation

a_i = coefficient in the coverage expansion of the available surface function
$a(r,r')$ = excluded area by a particle of radius r to one of radius r'
c_0 = bulk concentration
C_0 = characteristic bulk concentration
k = relative rate of desorption
k_a = adsorption rate constant
k_d = desorption rate constant
m = particle mass
m_p = pth moment of surface distribution
n_p = pth moment of bulk distribution
s = rescaled time

Greek letters

δ = fluctuation in surface size distribution
θ = surface coverage
μ = exponent in adsorption rate
ν = exponent in desorption rate
$\rho(r,t)$ = surface density
$\phi(r,t)$ = available surface function
$\chi_a(T)$ = temperature factor in adsorption rate
$\chi_d(T)$ = temperature factor in desorption rate

Literature Cited

Allen, M. P., and D. J. Tildesley, *Computer Simulation of Liquids*, Oxford University Press (1987).

Feder, J., "Random Sequential Adsorption," *Theor. Biol.*, **87**, 237 (1980).

Hinrichsen, E. L., J. Feder, and T. Jossang, "Geometry of Random Sequential Adsorption," *J. Stat. Phys.*, **44**, 793 (1986).

Hirtzel, C. S., and R. Rajagopalan, *Colloidal Phenomena Advanced Topics*, Noyes Publications, Park Ridge, NJ (1985).

Meakin, P., and R. Jullien, "Random Sequential Adsorption of Disks at Different Sizes," *Phys. Rev. A.*, **46**, 2029 (1992).

Schaaf, P., and J. Talbot, "Surface Exclusion Effects in Adsorption Processes," *J. Chem. Phys.*, **91**, 4401 (1989).

Talbot, J., and P. Schaaf, "Random Sequential Adsorption of Mixtures," *Phys. Rev. A.*, **40**, 422 (1989).

Tarjus, G., P. Schaaf, and J. Talbot, "Random Sequential Addition: A Distribution Function Approach," *J. Stat. Phys.*, **63**, 167 (1991).

Tarjus, G., and J. Talbot, "Random Sequential Adsorption of Polydisperse Mixtures: Asymptotic Kinetics and Structure," *J. Phys. A: Math Gen.*, **24**, L913 (1991).

Ugelsstad, J., A. Berge, R. Schmidt, P. Stenstad, and A. T. Skjeltorp, *Polymer Reaction Engineering*, H. Reichert and W. Geiseler, eds., Huthig and Wepf, Heidelberg (1986).

Van de Ven, T. G. M., *Colloidal Hydrodynamics*, Academic Press (1989).

Widom, B., "Random Sequential Addition of Hard Spheres to a Volume," *J. Chem. Phys.*, **44**, 3888 (1966).

Appendix

For some applications, it may be convenient to use a dimensionless form of Eq. 3. This may be achieved with the following quantities:

$$C_0 = \int_0^\infty c_0(r)dr, \quad R = \frac{1}{C_0}\int_0^\infty rc_0(r)dr, \quad \tilde{t} = \frac{R}{k_d(R)} \tag{A1}$$

Using the dimensionless concentrations:

$$c_0^*(r^*) = \frac{c_0(r)R}{C_0}, \quad \rho^*(r^*,t^*) = \frac{\rho(r,t)}{C_0}$$

and the dimensionless time $t^* = t/\tilde{t}$, where $r^* = r/R$, one may rewrite Eq. 3 as:

$$\frac{\partial \rho^*(r^*;t^*)}{\partial t^*} = k_a^*(r^*)c_0^*(r^*)\phi(r^*;t^*) - k_d^*(r^*)\rho^*(r^*;t^*) \qquad \text{(A2)}$$

where

$$k_a^*(r^*) = \frac{k_a(r)}{k_a(R)}, \quad k_d^*(r)^* = \frac{Rk_d(r)}{k_a(R)}$$

It is easy to show that the dimensionless distributions must satisfy the following relations:

$$\int_0^\infty c_0^*(r^*)dr^* = 1 \qquad \text{(A3)}$$

and

$$\int_0^\infty r^*c_0^*(r^*)dr^* = 1 \qquad \text{(A4)}$$

For example, if the polydispersity of a latex sphere solution can be described by:

$$c_0(r) = are^{-\lambda r} \qquad \text{(A5)}$$

for which $C_0 = a/\lambda^2$, $R = 2/\lambda$, then one need only consider the dimensionless distribution:

$$c_0^*(r^*) = 4r^*e^{-2r^*} \qquad \text{(A6)}$$

Manuscript received Oct. 13, 1992, and revision received Feb. 11, 1993.

Erratum

In the article titled "Robust Design of Binary Countercurrent Adsorption Separation Processes" (March 1993, p. 471), an incorrect Figure 8 (p. 480) was placed inadvertently. Here is the correct figure:

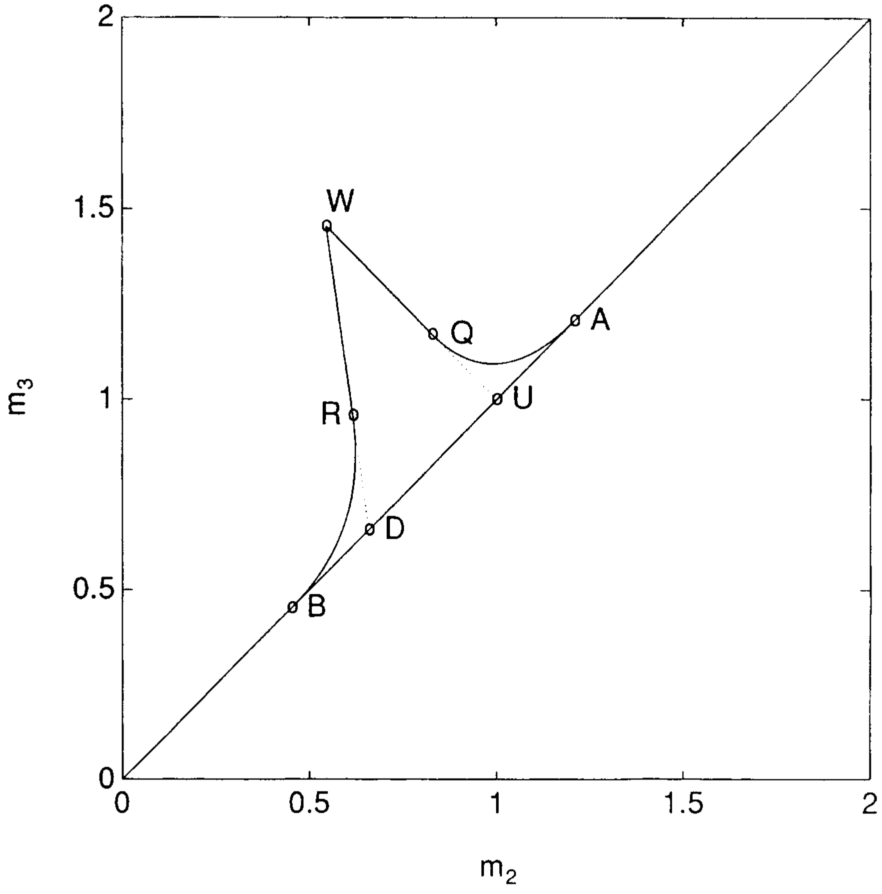

Figure 8. Region of complete separation in the $m_2 - m_3$ plane, in the case where $\Omega_F < K_D$. $K_A = 2.67$, $K_B = 1$, $K_D = 2.21$, $y_A^F = 0.5$, $y_B^F = 0.5$, $\Omega_F = 1.46$.